Stability enhancement of cytochrome *c* through heme deprotonation and mutations

Takafumi Sonoyama[a], Jun Hasegawa[b], Susumu Uchiyama[c], Shota Nakamura[d], Yuji Kobayashi[d], Yoshihiro Sambongi[a,*]

[a]*Graduate School of Biosphere Science, Hiroshima University, CREST of Japan Science and Technology Corporation, 1-4-4 Kagamiyama, Higashi-Hiroshima, Hiroshima 739-8528, Japan*

[b]*Daiichi Pharmaceutical Co., Ltd., 1-16-13 Kita-Kasai, Edogawa-ku, Tokyo 134-8630, Japan*

[c]*Graduate School of Engineering, Osaka University, Suita, Osaka 565-0871, Japan*

[d]*Graduate School of Pharmaceutical Science, Osaka University, Suita, Osaka 565-0871, Japan*

*Corresponding author. Tel. & Fax: +81 824 24 7924.

E-mail address: sambongi@hiroshima-u.ac.jp (Y. Sambongi)

Abbreviations: GdnHCl, guanidine hydrochloride; PA c_{551}, cytochrome c_{551} from *Pseudomonas aeruginosa*; CD, circular dichroism

Abstract

The chemical denaturation of *Pseudomonas aeruginosa* cytochrome c_{551} variants was examined at pH 5.0 and 3.6. All variants were stabilized at both pHs compared with the wild-type. Remarkably, the variants carrying the F34Y and/or E43Y mutations were more stabilized than those having the F7A/V13M or V78I ones at pH 5.0 compared with at pH 3.6 by ~3.0 – 4.6 kJ/mol. Structural analyses predicted that the side chains of introduced Tyr-34 and Tyr-43 become hydrogen donors for the hydrogen bond formation with heme 17-propionate at pH 5.0, but less efficiently at pH 3.6, because the propionate is deprotonated at the higher pH. Our results provide an insight into a stabilization strategy for heme proteins involving variation of the heme electronic state and introduction of appropriate mutations.

Keywords: Circular dichroism spectroscopy; Cytochrome *c*; Hydrogen bond; Protein stability; Heme propionate

1. Introduction

In order to enhance protein stability by protein engineering methods, one must find target regions in proteins that should be improved, and select candidate amino acid residues to be introduced. In this context, one can learn much on pair-wise comparison of highly homologous proteins isolated from thermophilic and mesophilic bacteria [1, 2]. After such comparison, mutagenesis work revealed many structural strategies for enhancing protein stability [3, 4]. For example, cytochrome *c* [5, 6], rubredoxin [7], ribonuclease H [8], adenylate kinase [9, 10], and cold shock protein [11, 12] have been studied in this way.

We have investigated the relationship between protein stability and structure using homologous mono-heme cytochromes *c* from mesophilic and thermophilic bacteria [5]. Cytochrome c_{551} (PA c_{551}) from a mesophile, *Pseudomonas aeruginosa*, and cytochrome c_{552} (HT c_{552}) from a thermophile, *Hydrogenobacter thermophilus*, are 82 and 80 amino acid proteins, respectively, each having a covalently attached heme. These proteins exhibit 56 % sequence identity and almost the same three-dimensional main chain conformation [13], but PA c_{551} shows lower stability than HT c_{552} [14].

After a careful survey of the side-chain interactions between the three-dimensional structures of HT c_{552} and PA c_{551}, we hypothesized that five residues, Ala-7, Met-13, Tyr-34, Tyr-43, and Ile-78, in the former are responsible for the higher stability mainly through the formation of more tightly packed hydrophobic cores [13]. A series of PA c_{551} variants having one to five of these residues at the corresponding positions (originally Phe-7, Val-13, Phe-34, Glu-43, and Val-78 in PA c_{551}) showed enhanced stability compared with the wild-type [15, 16].

Among the PA c_{551} variants used in our previous study, the variant with the F34Y/E43Y double mutations exhibited significantly different pH dependence in the redox potential value, as compared with the other variants and wild-type [17]. This difference should

be due to the difference in heme protonation/deprotonation behavior, since the pK_a value for the heme 17-propionate of this variant was around 4, which was at least 2 pH units lower than that of the wild-type [17].

In contrast to analysis of the pH-dependent redox potential of the PA c_{551} variants, that for stability has not been measured, and little is known whether there is any relationship between the heme electronic state and stability in PA c_{551}. Here, we show the stability of PA c_{551} variants including the F34Y and E43Y mutations at two different pHs, one below and one above 4. The results are compared with those for the other variants and the wild-type, which demonstrates that pH-dependent hydrogen bond formation between the introduced Tyr residues and the heme propionate contributes to the protein stability.

2. Materials and methods

2.1. Protein preparation.

The PA c_{551} wild-type and its variants used in this study were prepared as described previously [15, 16]. The protein concentrations were determined by spectrophotometric measurement after reduction with a sufficient amount of sodium dithionite [15].

2.2. Guanidine hydrochloride-induced denaturation.

Guanidine hydrochloride (GdnHCl)-induced denaturation of the air-oxidized PA c_{551} wild-type protein and its variants was monitored using a circular dichroism (CD)

spectropolarimeter with a Jasco J-820. Protein samples (20 μM) were incubated in 20 mM sodium acetate buffer (pH 5.0 or 3.6) with various concentrations of GdnHCl at 25 °C for two hours before the measurements in order to equilibrate the proteins with the denaturant. The GdnHCl concentrations were determined using the refractive index measured with a refractometer (Reichert, Inc., USA). The CD ellipticity at 222 nm of the protein solutions was measured at 25 °C in cuvettes of 1 mm path-length.

Data points (CD ellipticity plotted as a function of the GdnHCl concentration) were corrected for the slope of the baselines for the native and denatured forms, and normalized to calculate the fraction of protein denatured (examples are shown in Figs. 1 and 2). The fraction denatured was again plotted as a function of the GdnHCl concentration. Nonlinear least-squares fitting of the normalized data was performed according to the previously described method [15]. The resulting GdnHCl-induced denaturation profiles were analyzed using a two-state model, and the difference in the Gibbs free energy change between the native and denatured states (ΔG) was calculated as described by Pace [18]. The free energy change in water (ΔG_{H2O}) and the dependence of ΔG on the GdnHCl concentration (m) were determined by least-squares fitting of the data in the transition region using the equation: $\Delta G = \Delta G_{H2O} - m$[GdnHCl]. The midpoint of the GdnHCl denaturation (C_m) was taken as the concentration of GdnHCl at which the ΔG value became zero.

3. Results and discussion

3.1. Stability against GdnHCl-induced denaturation

Figure 1 shows the results of GdnHCl-induced denaturation obtained at pH 5.0. CD ellipticity at 222 nm was plotted as a function of the GdnHCl concentration (Fig. 1A), which was then normalized to calculate the fraction of denatured protein (Fig. 1B). The denaturation curves could be adequately fitted to a two-state model for protein denaturation, because the curves obtained in the present experiments were S-shaped and the previous kinetic experiments demonstrated the absence of an intermediate during denaturation of the PA c_{551} wild-type [19].

The normalized denaturation curves provided the C_m values for the PA c_{551} wild-type, and the variants carrying the F7A/V13M, F34Y, E43Y, F34Y/E43Y, V78I, F7A/V13M/F34Y/E43Y, F7A/V13M/V78I, F34Y/E43Y/V78I, and F7A/V13M/F34Y/E43Y/V78I mutations (Table 1). The C_m values of all the variants examined in this study were larger than that of the wild-type. The stability of each variant was also evaluated as the ΔG_{H2O} value (Table 1), which had been estimated and extrapolated from the dependence of ΔG on the GdnHCl concentration in the transition region (Fig. 1C). The resulting ΔG_{H2O} values showed that the mutations caused enhanced stabilization of PA c_{551} at pH 5.0.

Figure 2 shows the results of GdnHCl-induced denaturation obtained at pH 3.6. The data obtained were processed similarly to those at pH 5.0 described above. The normalized GdnHCl denaturation profiles obtained at pH 3.6 (Fig. 2B) gave C_m values showing that all the variants were stabilized compared with the wild-type PA c_{551} (Table 1). From the extrapolation (Fig. 2C), ΔG_{H2O} values were also calculated, which showed that all the

mutation(s) caused enhanced stabilization of PA c_{551} against GdnHCl at pH 3.6 (Table 1).

3.2. Stability comparison between pH 5.0 and 3.6

We also carried out GdnHCl denaturation experiments at pH 3.0, but the wild-type and some variants started to undergo denaturation at the lower GdnHCl concentration (< 0.5 M), and thus precise denaturation profiles could not be obtained. Therefore, we compared the stability against GdnHCl denaturation at pH 5.0 and 3.6 in order to evaluate the pH effect. For all the PA c_{551} variants examined, the C_m value of one protein measured at pH 5.0 was larger than that of the same protein at pH 3.6 (Table 1). These results indicated that the lower pH had a negative effect on the protein stability.

Figure 3 shows plots of the $\Delta\Delta G_{H2O}$ value of each protein on a matrix with axes of the two different pHs. The plots of the variants having the F34Y/E43Y mutations such as the F34Y/E43Y, F7A/V13M/F34Y/E43Y, F34Y/E43Y/V78I, and F7A/V13M/F34Y/E43Y/V78I ones were on the same linear correlation curve (closed symbols in Fig. 3), while those of the wild-type, and the F7A/V13M, V78I, and F7A/V13M/V78I variants, which did not have the F34Y/E43Y mutations, were on the other curve (open symbols in Fig. 3). The plots of the F34Y and E43Y variants (x and + marks, respectively, in Fig. 3) were intermediate between those of these two groups. This grouping showed that the variants having the F34Y and E43Y mutations, or both exhibited more enhanced stability at pH 5.0 than at pH 3.6 compared with the variants without these mutations.

The above grouping was quantitatively evaluated as follow. First, the $\Delta\Delta G_{H2O}$ value of each variant obtained at pH 3.6 was subtracted from that of the same protein obtained at pH 5.0

(Table 2). This calculation showed that the variants having the F34Y/E43Y mutations were stabilized at pH 5.0 on average by 5.95 kJ/mol (‘average +F34Y/E43Y mutations’ in Table 2) compared with those at pH 3.6. Similarly, the variants with the single F34Y and E43Y mutations exhibited stability enhancement of 4.42 and 4.35 kJ/mol, respectively. In contrast, the wild-type and the variants without the F34Y/E43Y mutations were stabilized at pH 5.0 by only 1.37 kJ/mol on average compared with at pH 3.6 (‘average -F34Y/E43Y mutations’ in Table 2).

Next, further deduction of the value of ‘average -F34Y/E43Y mutations’ from that of ‘average +F34Y/E43Y mutations’ resulted in the value of 4.58 kJ/mol. This value represents the strength of the interaction caused by the F34Y/E43Y mutations, which appears at pH 5.0, but not at pH 3.6. Similarly, deduction of the value of ‘average -F34Y/E43Y mutations’ from those of F34Y and E43Y in Table 2 resulted in ~3.0 kJ/mol. These values will be discussed below.

3.3. Structural features on hydrogen bond formation

The effects of the F34Y and E43Y mutations in PA c_{551} can be attributed to the formation of hydrogen bonds with the heme, as judged on crystal structure comparison between PA c_{551} [20] and the thermophilic counterpart, HT c_{552} [21]. This structural comparison was possible because of two reasons: first, the two cytochromes *c* have almost identical main chain conformations, and second, the interactions between side-chains can be easily estimated. In particular, the only difference in the side chains between Phe and Tyr, found at position 34 in the two proteins, is the existence of an OH group (Fig. 4). The crystal structure of HT c_{552} [21] has revealed that the η O atoms of the two Tyr residues at positions 34 and 43 are hydrogen-bonded

to O-1A and O-2A of the heme 17-propionate, respectively (Fig. 4). In the case of the PA c_{551} wild-type crystal structure [20], the corresponding Phe-34 and Glu-43 do not form hydrogen bonds (Fig. 4).

Our present stability analysis, as discussed in the previous section, showed that the stabilization strength caused by the single F34Y and E43Y mutations was 3.0 kJ/mol, in accordance with the pH difference, and was thus comparable to the average value of ~4 kJ/mol per hydrogen bond as to the stabilization of globular proteins [22]. For the double F34Y/E43Y mutations, however, the corresponding value was 4.6 kJ/mol, which was about half as to the energy for two hydrogen bonds. This suggests that each of the F34Y and E43Y mutations does not additively contribute to the stability enhancement around this region.

3.4. Effect of heme deprotonation on hydrogen bond formation

The previous paramagnetic NMR study can explain the present observation of different contributions of the F34Y/E43Y mutations to the protein stability at pH 5.0 and 3.6. The pK_a values attributed to protonation/deprotonation of the heme 17-propionate of the wild-type and F7A/V13M/V78I variant were each 6.1, whereas that of the F34Y/E43Y variant was around 4 [17]. We can then assume that the heme 17-propionate of the variants having the F34Y/E43Y mutations has a greater chance to be deprotonated at pH 5.0 than at pH 3.6. Since the Tyr side chain is assumed to be protonated (the pK_a value for its phenol is 10.46) at pH 5.0, heme deprotonation at pH 5.0 results in the formation of a hydrogen bond between Tyr-34 and/or Tyr-43 (as hydrogen donors), and the heme (as a hydrogen acceptor).

4. Conclusions

We experimentally proved the contribution of pH-dependent hydrogen bond formation to the stability of PA c_{551}. This finding represents a consequence of the chemical interactions between Tyr-34 and/or Tyr-43, and the heme that have been previously shown to affect the redox potential. The present stabilization strategy, which involves the naturally occurring stable counterpart HT c_{552}, can be accomplished by selecting appropriate pH conditions and mutations in the less stable PA c_{551}, thus providing guidelines for designing more stable heme proteins.

Acknowledgment

This work was partly supported by a grant from the Japanese Ministry of Education, Science and Culture (Grant-in-Aid for Scientific Research on Priority Areas).

References

[1] A. Razvi, J.M. Scholtz, Lessons in stability from thermophilic proteins, Protein Sci. 15 (2006) 1569–1578.

[2] R. Jaenicke, Stability and stabilization of globular proteins in solution, J. Biotechnol. 79, (2000) 193–203.

[3] C. Vieille, G. J. Zeikus, Hyperthermophilic enzymes: sources, uses, and molecular mechanisms for thermostability, Microbiol. Mol. Biol. Rev. 65 (2001) 1-43.

[4] B. van den Burg, V.G.H. Eijsink, Selection of mutations for increased protein stability, Curr. Opin. Biotechnol. 13 (2002) 333-337.

[5] Y. Sambongi, S. Uchiyama, Y. Kobayashi, Y. Igarashi, J. Hasegawa, Cytochrome *c* from a thermophilic bacterium has provided insights into the mechanism of protein maturation, folding, and stability, Eur. J. Biochem. 269 (2002) 3355-3361.

[6] C. Lange, I. Luque, M. Hervas, J. Ruiz-Sanz, P.L. Mateo, M.A. De la Rosa, Role of the surface charges D72 and K8 in the function and structural stability of the cytochrome c_6 from *Nostoc* sp. PCC 7119, FEBS J. 272 (2005) 3317-3327.

[7] D.M. LeMaster, G. Hernández, Residue cluster additivity of thermodynamic stability in the hydrophobic core of mesophile vs. hyperthermophile rubredoxins, Biophys. Chem. 125 (2007) 483-489.

[8] N. Ohtani, M. Haruki, M. Morikawa, S. Kanaya, Heat labile ribonuclease HI from a psychrotrophic bacterium: gene cloning, characterization and site-directed mutagenesis, Protein Eng. 14 (2001) 975-982.

[9] P.J. Haney, M. Stees, J. Konisky, Analysis of thermal stabilizing interactions in mesophilic and thermophilic adenylate kinases from the genus *Methanococcus*, J. Biol. Chem. 274, (1999) 28453-28458.

[10] A.R. Criswell, E. Bae, B. Stec, J. Konisky, G.N. Phillips Jr., Structures of thermophilic and mesophilic adenylate kinases from the genus *Methanococcus*, J. Mol. Biol. 330 (2003) 1087-1099.

[11] D. Perl, U. Müller, U. Heinemann, F.X. Schmid, Two exposed amino acid residues confer thermostability on a cold shock protein, Nat. Struct. Biol. 7 (2000) 380–383.

[12] A. Martin, I. Kather, F.X. Schmid, Origins of the high stability of an in vitro-selected cold-shock protein, J. Mol. Biol. 318 (2002) 1341-1349.

[13] J. Hasegawa, T. Yoshida. T. Yamazaki, Y. Sambongi, Y. Yu, Y. Igarashi, T. Kodama, K. Yamazaki, Y. Kyogoku, Y. Kobayashi, Solution structure of thermostable cytochrome *c*-552 from *Hydrogenobacter thermophilus* determined by ^{1}H-NMR spectroscopy, Biochemistry 37 (1998) 9641-9649.

[14] Y. Sanbongi, Y. Igarashi, T. Kodama, Thermostability of cytochrome *c*-552 from the thermophilic hydrogen-oxidizing bacterium *Hydrogenobacter thermophilus*, Biochemistry 28 (1989) 9574-9578.

[15] J. Hasegawa, H. Shimahara, M. Mizutani, S. Uchiyama, H. Arai, M. Ishii, Y. Kobayashi, S.J. Ferguson, Y. Sambongi, Y. Igarashi, Stabilization of *Pseudomonas aeruginosa* cytochrome *c*-551 by systematic amino acid substitutions based on the structure of thermophilic *Hydrogenobacter thermophilus* cytochrome *c*-552, J. Biol. Chem. 274 (1999) 37533-37537.

[16] J. Hasegawa, S. Uchiyama, Y. Tanimoto, M. Mizutani, Y. Kobayashi, Y. Sambongi, Y. Igarashi, Selected mutations in a mesophilic cytochrome *c* confer the stability of a thermophilic counterpart, J. Biol. Chem. 275 (2000) 37824-37828.

[17] S.J. Takayama, M. Mikami, N. Terui, H. Mita, J. Hasegawa, Y. Sambongi, Y. Yamamoto, Control of the redox potential of *Pseudomonas aeruginosa* cytochrome c_{551} through the

Fe-Met coordination bond strength and pK_a of a buried heme propionic acid side chain, Biochemistry 44 (2005) 5488-5494.

[18] C.N. Pace, Measuring and increasing protein stability, Trends Biotechnol. 8 (1990) 93-98.

[19] S. Gianni, C. Travaglini-Allocatelli, F. Cutruzzolà, M.G. Bigotti, M. Brunori, Snapshots of protein folding. A study on the multiple transition state pathway of cytochrome c_{551} from *Pseudomonas aeruginosa*, *J. Mol. Biol*. 309 (2001) 1177-1187.

[20] Y. Matsuura, T. Takano, R.E. Dickerson, Structure of cytochrome c_{551} from *Pseudomonas aeruginosa* refined at 1.6 Å resolution and comparison of the two redox forms, J. Mol. Biol. 156 (1982) 389-409.

[21] C. Travaglini-Allocatelli, S. Gianni, V.K. Dubey, A. Borgia, A. Di Matteo, D. Bonivento, F. Cutruzzola, K.L. Bren, M. Brunori, An obligatory intermediate in the folding pathway of cytochrome c_{552} from *Hydrogenobacter thermophilus*, J. Biol. Chem. 280 (2004) 25729-25734.

[22] J.K. Myers, C.N. Pace, Hydrogen bonding stabilizes globular proteins, Biophys. J. 71 (1996) 2033-2039.

Figure legends

Fig. 1. Stability against GdnHCl-induced denaturation at pH 5.0. (A) CD ellipticity values are plotted as a function of the GdnHCl concentration with the fitting curves. (B) Normalized fractions of protein denatured are plotted as a function of the GdnHCl concentration with the fitting curves. (C) ΔG values are are plotted as function of the GdnHCl concentration with the fitting curves. Symbols: Wild-type (open circles), F7A/V13M variant (open triangles), F34Y variant (x), E43Y variant (+), F34Y/E43Y variant (closed circles), V78I variant (open squares), F7A/V13M/F34Y/E43Y variant (closed triangles), F7A/V13M/ V78I variant (open diamonds), F34Y/E43Y/V78I variant (closed squares), and F7A/V13M/F34Y/E43Y/V78I variant (closed diamonds).

Fig. 2. Stability against GdnHCl-induced denaturation at pH 3.6. (A) CD ellipticity values are plotted as a function of the GdnHCl concentration with the fitting curves. (B) Normalized fractions of protein denatured are plotted as a function of the GdnHCl concentration with the fitting curves. (C) ΔG values are are plotted as a function of the GdnHCl concentration with the fitting curves. The symbols representing the variants are the same as in Fig. 1.

Fig. 3. Stability comparison between pH 5.0 and 3.6 during GdnHCl denaturation. The $\Delta\Delta G_{H2O}$ values obtained at pH 5.0 and 3.6 are plotted. On the matrix, the 45-degree line (dotted) shows that the enhanced stabilities compared to those of the wild-type at the two pHs are the same, and the plots in the upper region show that the stability at pH 5.0 is greater than that at pH 3.6. GdnHCl denaturation experiments were carried out independently at least three times, and standard deviations are shown by bars. The symbols representing the variants are the same as in Fig. 1.

Fig. 4. Formation of a hydrogen bond. The three-dimensional crystal structures of parts of the PA c_{551} wild-type and HT c_{552} are compared. Interactions between the heme group, and the amino acid side-chains at positions 34 and 43 in HT c_{552} are shown together with the distances between the η oxygen atoms of the Tyr residues and the oxygen atoms of the heme 17-propionate. The PDB numbers are 451C (PA c_{551}) and 1YNR (HT c_{552}).

Fig. 1

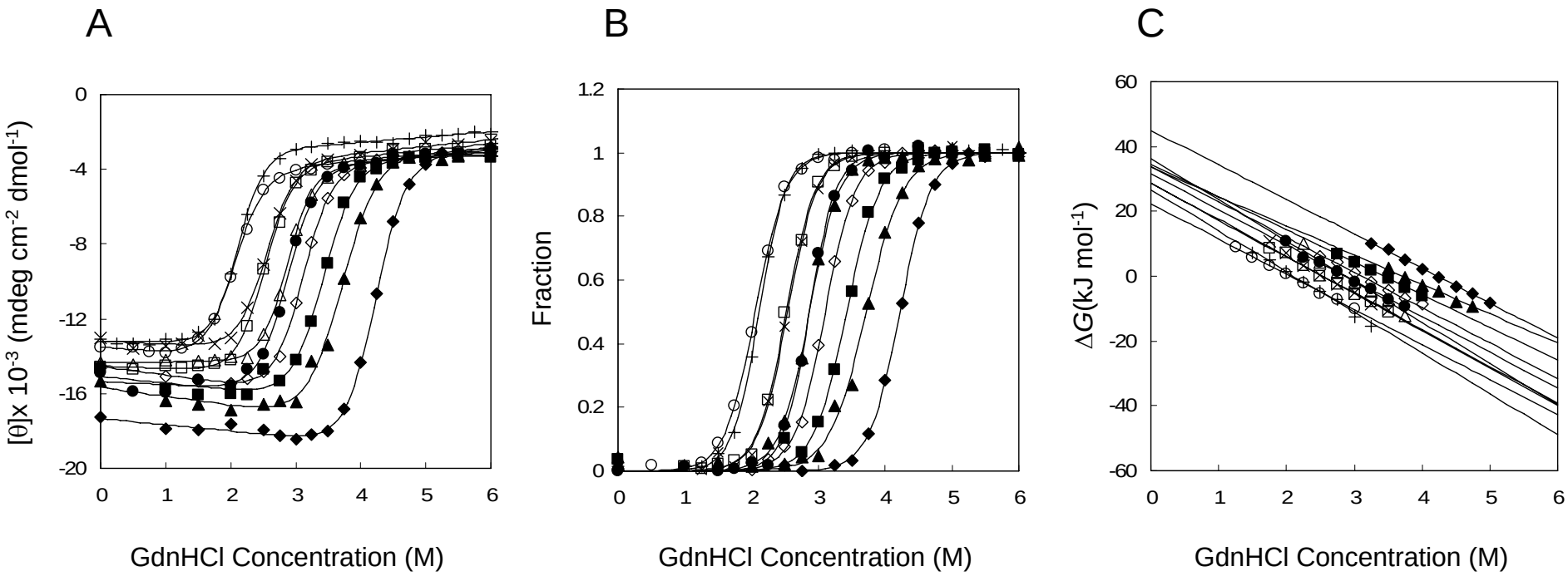
A
B
C
[θ]x 10-3 (mdeg cm-2 dmol-1)
Fraction
ΔG(kJ mol-1)
GdnHCl Concentration (M)
GdnHCl Concentration (M)
GdnHCl Concentration (M)

Fig. 2

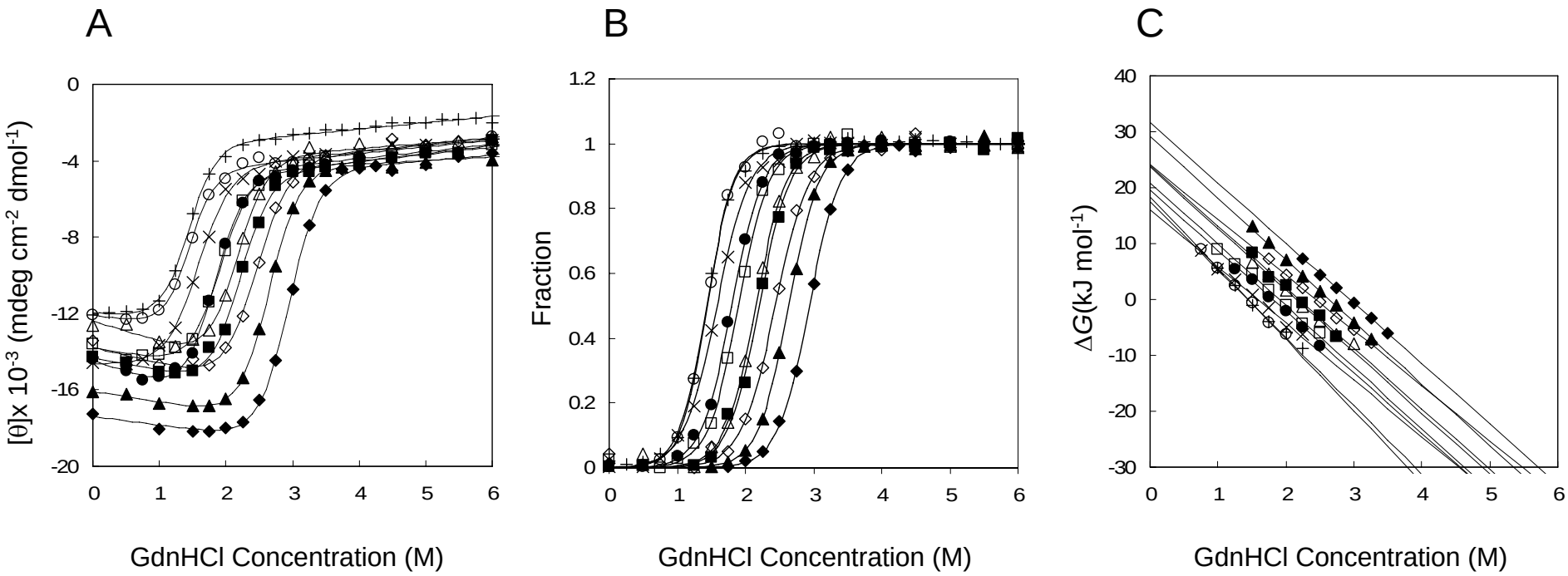
A
B
C
[θ]x 10-3 (mdeg cm-2 dmol-1)
Fraction
ΔG(kJ mol-1)
GdnHCl Concentration (M)
GdnHCl Concentration (M)
GdnHCl Concentration (M)

Fig. 3

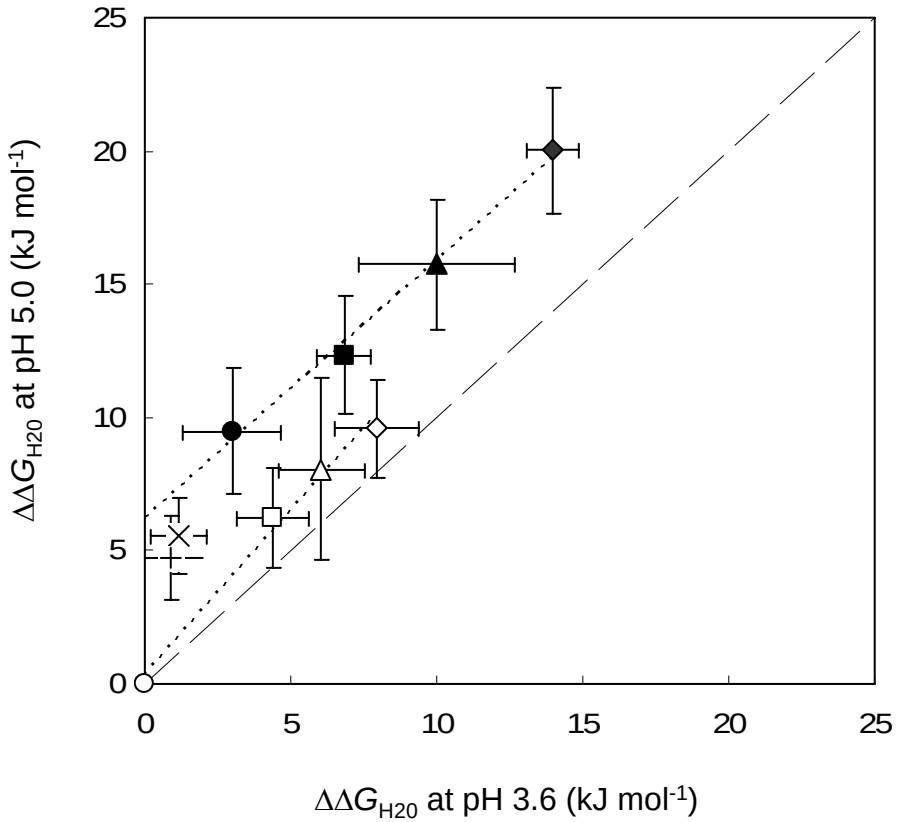
25
20
15
10
5
0
0
5
10
15
20
25
ΔΔG_H20 at pH 5.0 (kJ mol-1)
ΔΔG_H20 at pH 3.6 (kJ mol-1)

Fig. 4.

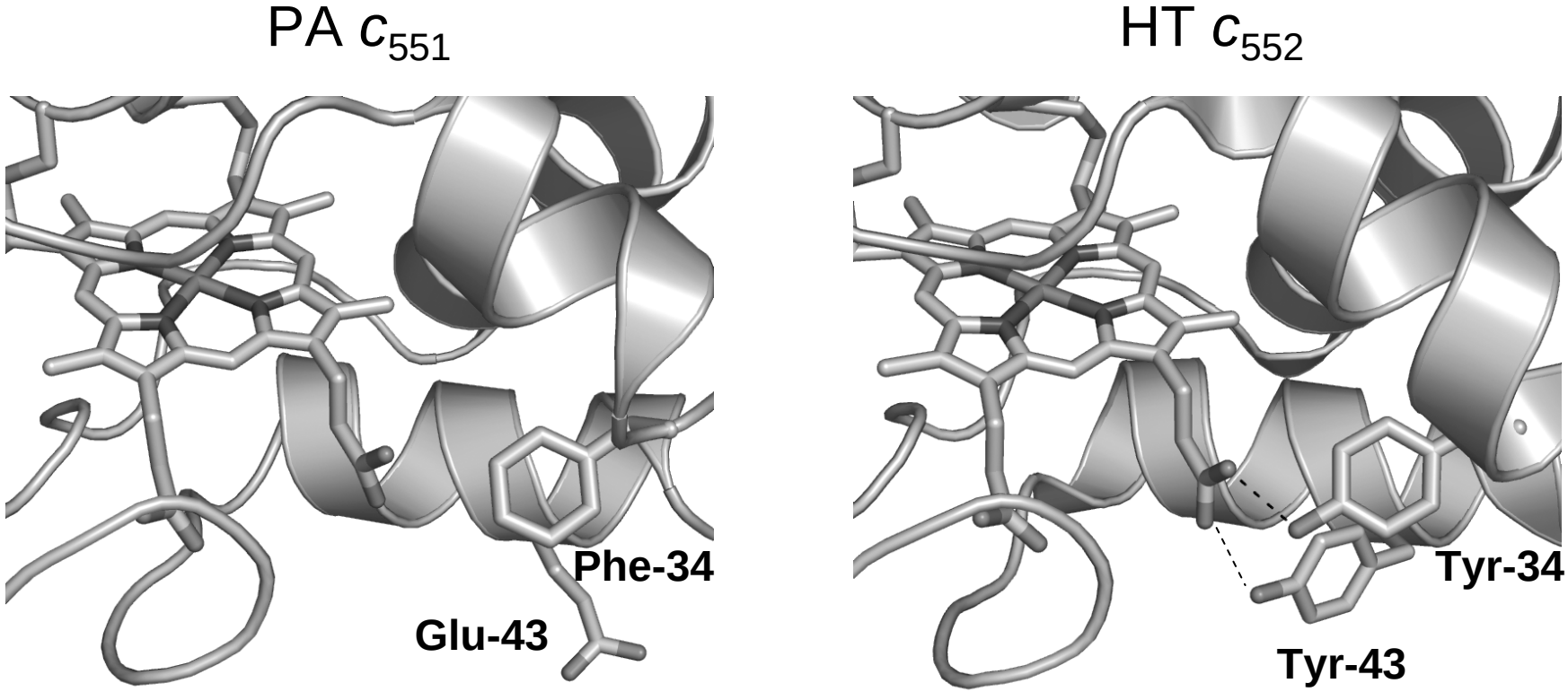

Table 1

Parameters characterizing the GdnHCl-induced denaturation of PA c_{551} variants

Protein	pH 5.0		
	C_m (ΔC_m)	*m*	ΔG_{H20} ($\Delta\Delta G_{H2O}$)
	M	*kJ/mo/M*	*kJ/mol*
Wild type	2.06 ± 0.01 (0)	11.05 ± 0.61	22.78 ± 1.33 (0)
F7A/V13M	2.87 ± 0.02 (0.81)	10.76 ± 1.14	30.83 ± 3.14 (8.05)
F34Y	2.54 ± 0.02 (0.48)	11.16 ± 0.15	28.35 ± 0.55 (5.58)
E43Y	2.12 ± 0.02 (0.06)	12.99 ± 0.39	27.50 ± 0.67 (4.72)
F34Y/E43Y	2.88 ± 0.01 (0.82)	11.22 ± 0.79	32.27 ± 2.23 (9.49)
V78I	2.53 ± 0.01 (0.47)	11.46 ± 0.54	29.00 ± 1.34 (6.22)
F7A/V13M/F34Y/E43Y	3.78 ± 0.08 (1.72)	10.18 ± 0.47	38.53 ± 2.05 (15.75)
F7A/V13M/V78I	3.13 ± 0.04 (1.07)	10.34 ± 0.38	32.37 ± 1.29 (9.59)
F34Y/E43Y/V78I	3.44 ± 0.03 (1.38)	10.20 ± 0.43	35.12 ± 1.81 (12.34)
F7A/V13M/F34Y/E43Y/V78I	4.20 ± 0.02 (2.14)	10.19 ± 0.42	42.80 ± 1.94 (20.02)

Protein	pH 3.6		
	C_m (ΔC_m)	*m*	ΔG_{H20} ($\Delta\Delta G_{H2O}$)
	M	*kJ/mo/M*	*kJ/mol*
Wild type	1.44 ± 0 (0)	12.06 ± 0.61	17.31 ± 0.84 (0)
F7A/V13M	2.18 ± 0.05 (0.74)	10.73 ± 0.77	23.36 ± 1.22 (6.05)
F34Y	1.60 ± 0.01 (0.17)	11.53 ± 0.35	18.47 ± 0.48 (1.15)
F34Y/E43Y	1.80 ± 0.03 (0.36)	11.29 ± 0.79	20.31 ± 1.70 (2.99)
E43Y	1.46 ± 0.05 (0.02)	12.06 ± 0.21	17.68 ± 0.82 (0.37)
V78I	1.89 ± 0.02 (0.46)	11.45 ± 0.49	21.69 ± 0.90 (4.38)
F7A/V13M/F34Y/E43Y	2.59 ± 0.04 (1.15)	10.54 ± 0.87	27.30 ± 2.53 (9.99)
F7A/V13M/V78I	2.46 ± 0.02 (1.02)	10.26 ± 0.42	25.26 ± 1.14 (7.94)
F34Y/E43Y/V78I	2.25 ± 0.04 (0.81)	10.75 ± 0.06	24.13 ± 0.34 (6.82)
F7A/V13M/F34Y/E43Y/V78I	2.95 ± 0.01 (1.52)	10.61 ± 0.14	31.30 ± 0.32 (13.98)

Measurements were independently carried out at least three times, and the values are presented as means ± standard deviation. The differences in C_m (ΔC_m) and ΔG_{H2O} ($\Delta\Delta G_{H2O}$) between the wild-type and variants were calculated by subtracting the wild-type values from those for the variants.

Table 2

Difference in $\Delta\Delta G_{H20}$ values between pH 5.0 and 3.6.

Protein	$\Delta\Delta G_{H20}$(pH 5.0)-$\Delta\Delta G_{H2O}$(pH 3.6)
	kJ/mol
Wild type	0.00
F7A/V13M	2.00
V78I	1.84
F7A/V13M/V78I	1.65
average -F34Y/E43Y mutations	1.37
F34Y/E43Y	6.49
F7A/V13M/F34Y/E43Y	5.76
F34Y/E43Y/V78I	5.52
F7A/V13M/F34Y/E43Y/V78I	6.04
average +F34Y/E43Y mutations	5.95
F34Y	4.42
E43Y	4.35